Targeted synthesis of regioisomerically pure dodecasubstituted type I porphyrins through the exploitation of *peri*-interactions

Marc Kielmann, Keith J. Flanagan, Mathias O. Senge*

School of Chemistry, SFI Tetrapyrrole Laboratory, Trinity Biomedical Sciences Institute, Trinity College Dublin, the University of Dublin, 152–160 Pearse St., Dublin 2, Ireland

Email: Mathias O. Senge - sengem@tcd.ie

* Corresponding author

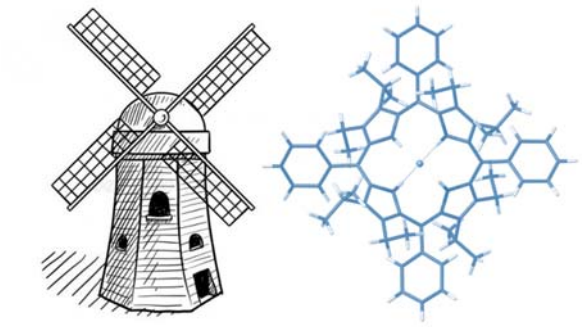

ABSTRACT: A targeted synthesis of dodecasubstituted type I porphyrins that utilizes the reaction of unsymmetrical 3,4-difunctionalized pyrroles and sterically demanding aldehydes was developed. This way, type I porphyrins could be obtained as the only type isomers, likely due to a minimization of the steric strain arising from *peri*-interactions. Uniquely, this method does not depend on lengthy precursor syntheses, the separation of isomers, or impractical limitations of the reaction scale. In addition, single crystal X-ray analysis elucidated the structural features of the macrocycles.

Porphyrins are abundant in nature where they fulfill many important roles, for example, in the functioning of pigment protein complexes and metalloproteins.[1,2] Today, they are frequently applied as model compounds to illustrate new achievements in multiple scientific areas, including biology, chemistry, medicine, physics, and beyond.[3] Conclusively, research aims to synthesize complex porphyrin architectures with diverse substitution patterns that show tailored functional properties, including organocatalytic activity,[4] singlet oxygen delivery,[5] and innovative sensors.[6] As such, short but efficient syntheses or new functionalization reactions are highly sought after.[7] However, the choice of which synthetic route to use to synthesize any particular porphyrin depends upon the symmetry features of the product itself.

The synthesis of regioisomerically enriched or pure porphyrin type isomers usually depends on the preparation of special pyrrolic precursors or the design of particular condensation strategies. That is because conventional condensation reactions of, e.g., 3,4-disubstituted pyrroles would result in the formation of statistical mixtures of all possible type isomers. Moreover, due to the very similar physicochemical properties of a set of type isomers, it is not trivial to separate these on a preparative scale. Thus, for example, etioporphyrin I (**1**) and coproporphyrin I tetramethyl ester are accessible by the tetramerization of α-functionalized pyrroles,[8] and so-called *opp*-porphyrins, in which like pyrrole rings are regiochemically situated opposite to each other, were prepared in a similar fashion.[9] On the other hand, dipyrromethenes have been utilized in the syntheses of **1** and coproporphyrin I (**5**) as well as to prepare regioisomerically pure etiobiliverdin IVγ, which is a bile pigment (Figure 1).[10]

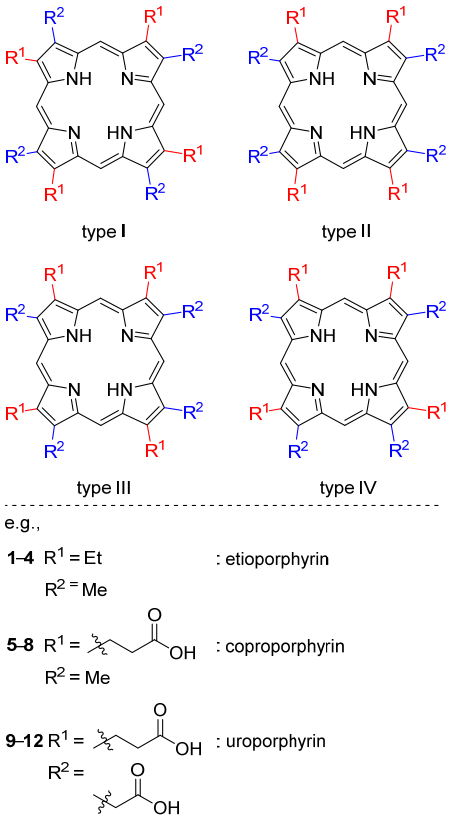

Figure 1: Examples of porphyrin type isomers: etioporphyrin I–IV (1–4) as well as biologically relevant copro- and uroporphyrin I–IV (5–8 and 9–12, respectively).

This methodology was later extended to the use of dipyrromethenes for the preparation of isomers other than type I.[11] At the same time, where the separation of type isomers from statistical mixtures is attempted, time-consuming or small-scale purification methods are required, such as HPLC. Naturally, this is more challenging the more type isomers are present in a given sample. Type I and III isomers of penta-, hexa-, and heptacarboxyporphyrin as well as those of uro- (**9** and **11**), copro- (**5** and **7**), and isocoproporphyrin were separated via HPLC.[12] The authors stated that this method would be suitable for the preparative isolation and for the detailed analysis of such isomers in clinical materials, e.g., urine and feces of patients. More recently, HPLC was also applied to separate coproporphyrin I and III (**5** and **7**) where tetrapyrroles were extracted from various types of yeast and bacteria and then analyzed by MS.[13]

Porphyrin type isomers[14] are important for medicinal and synthetic studies: In one report, tetrapyrroles excreted by patients with different types of porphyria were

analyzed.[15] Therein, the type isomer composition was disclosed with regards to, for example, type I and III uro- (**9** and **11**) and coproporphyrin (**5** and **7**) presence depending on the type of porphyria. On a different note, the synthetic value of all β-tetra(*tert*-butyl)porphyrin type isomers has been proven when they were used as precursors for porphyrine ("porphine"). Similar to 5,10,15,20-tetra(*tert*-butyl)porphyrin,[16] they could be tetradealkylated to give porphrine in good yield.[17] This is the parent structure of all porphyrins found in nature and therefore a synthetic target of immense importance for fundamental research.[18]

This overview shows that methods for the facile synthesis of regioisomerically pure porphyrin type isomers are scarce. Moreover, the synthetic approaches that were shown are usually not broadly applicable and as such, a relatively small library of such tetrapyrroles is at hand. This was taken as an occasion to elaborate a concept where simple Lindsey condensation reactions[19] would lead to the preferential formation of type I porphyrins (Scheme 1).

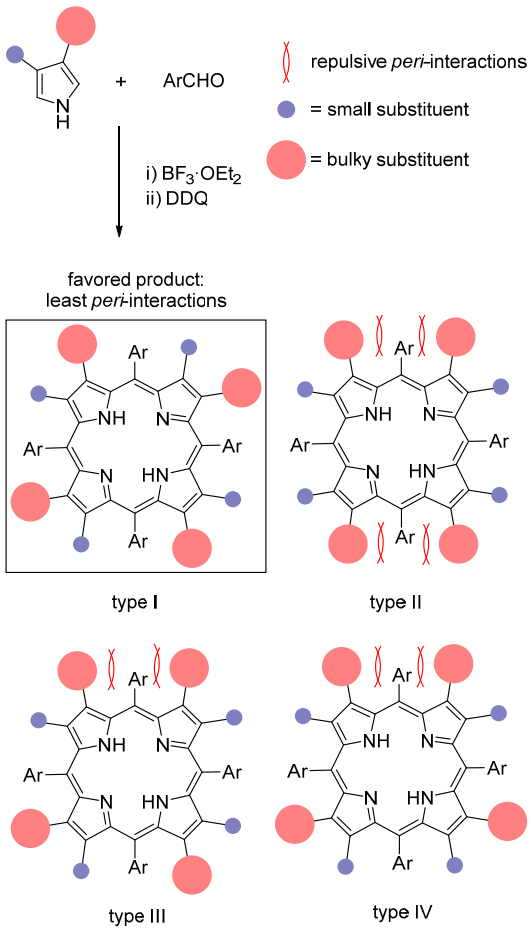

Scheme 1: Concept of the targeted synthesis of highly substituted type I porphyrins, rather than a statistical mixture, from unsymmetrical 3,4-difunctionalized pyrroles and sterically demanding aldehydes.

In this proposal, the pyrrolic precursors are designed in a way that a significant difference in steric demand between the groups carried at the 3- vs the 4-position is generated (e.g., as in **14**). When condensed with large aromatic aldehydes, type I porphyrins should be formed as the major products due to a minimization of the *peri*-interactions and the reduction of the overall steric strain. *peri*-Interactions are conformational effects that occur when meso residues are flanked by β substituents.[20] This creates a steric clash, resulting in high energy steric strain and deformation of the molecule, which is particularly pronounced in dodecasubstituted porphyrins.[21]
For proof of principle, 3-ethyl-4-isopropylpyrrole (**14**) was prepared by the reduction of 3-acetyl-4-isopropylpyrrole (**13**) with lithium aluminium hydride in 84% yield. And indeed, the following reaction of compound **14** with benzaldehyde in the presence of the Lewis acidic BF_3 catalyst yielded **15**•2HCl as the only detectable porphyrin species after the reduction with 2,3-dichloro-5,6-dicyano-1,4-benzoquinone (DDQ, Scheme 2). Notably, **15** was obtained as a dihydrochloride salt, as indicated by the presence of only two Q bands in the UV–vis absorption spectrum, due to the protonation by residual hydrochloric acid present in the solvent. This can be associated with the pronounced basicity of the neutral macrocycle **15** due to the high degree of nonplanarity and electron-rich character.[4c] However, for the purpose of this study, the neutralization of the complex was ultimately not attempted.

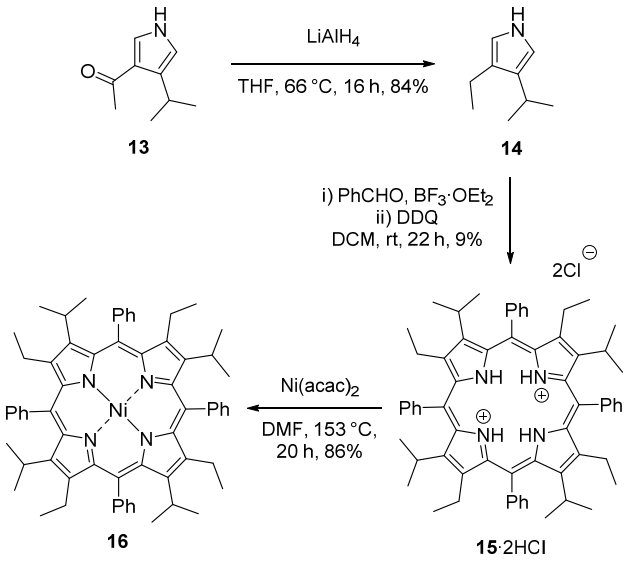

Scheme 2. Synthesis of type I porphyrin isomers 15•2HCl and 16 through condensation and metallation.

The formation of the type I isomer **15**·2HCl was confirmed with certainty by single crystal X-ray analysis. Interestingly, the alternating ethyl–isopropyl type I substituent pattern resulted in an overall molecular shape resembling a macroscopic propeller or a Dutch windmill where the isopropyl groups are analogous to molecular-scale blades attached at a precise 90° pitch angle. To investigate the features of the corresponding metalloporphyrin **16**, and for comparison with **15**•2HCl, Ni(II) insertion was performed, which occurred in a high yield of 86%. The crystal structures of both **15**•2HCl and the Ni(II) complex **16** revealed a severe saddle distortion of each macrocycle (Figure 2).

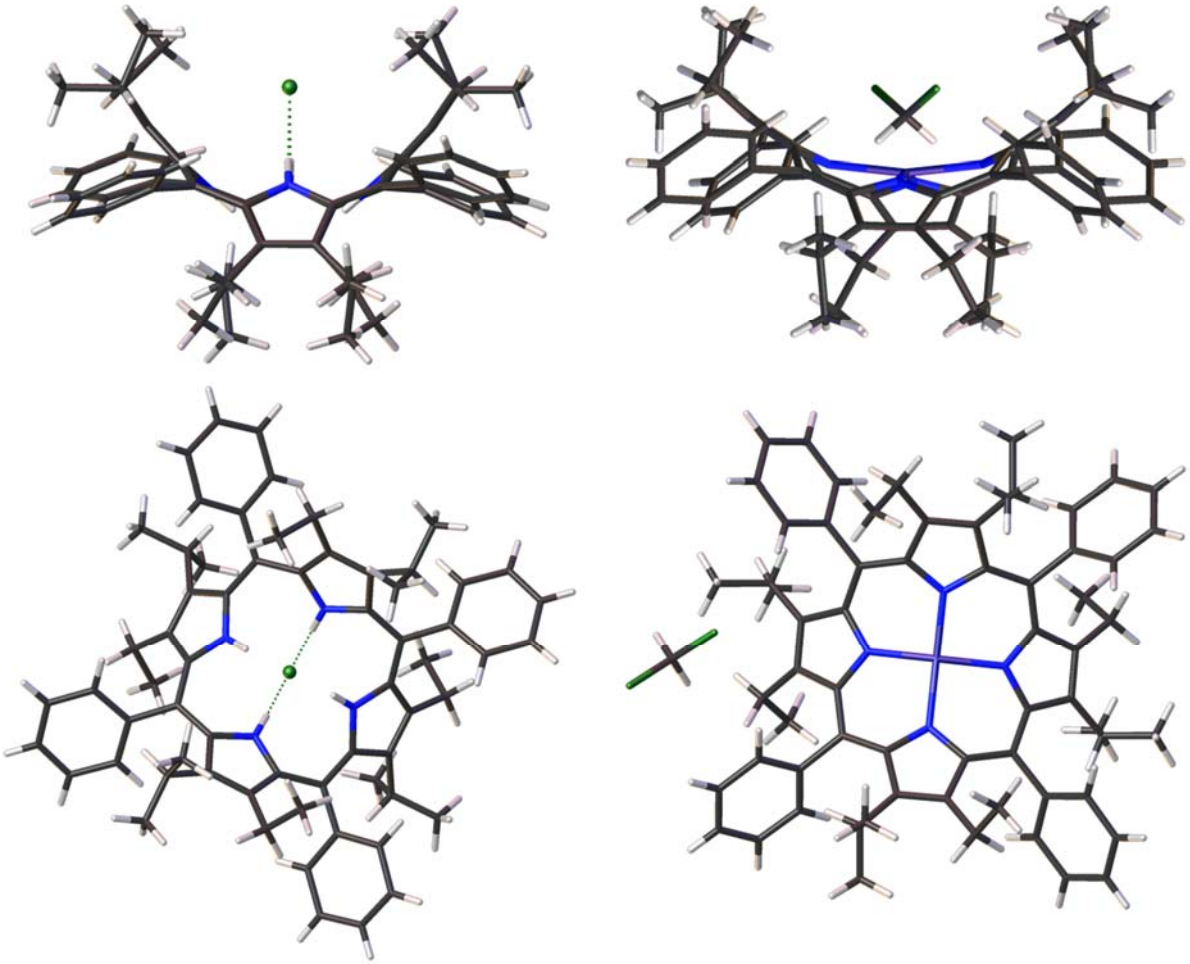

Figure 2: Side and top views (stick models) of 15•2HCl (left) and 16•DCM (right).[23a]

In addition, the crystal lattice of **16** had a tunnel-like structure where DCM was incorporated (Figure 3). Moreover, the isopropyl substituents extended well beyond the porphyrin plane, with the result that the DCM guest molecules were fully engulfed in hydrophobic binding pockets. The formation of this nonplanar metalloporphyrin solvate complex is somewhat reminiscent of {2,3,7,8,12,13,17,18-octaethyl-5,10,15,20-tetraphenylporphyrinato}copper(II) dichloromethane solvate (Cu(II)OETPP•2DCM) and points at possible receptor applications due to the availability of solvent-accessible voids[4a,22] or at enzyme-like catalytic properties due to the presence of hydrophobic cavities.

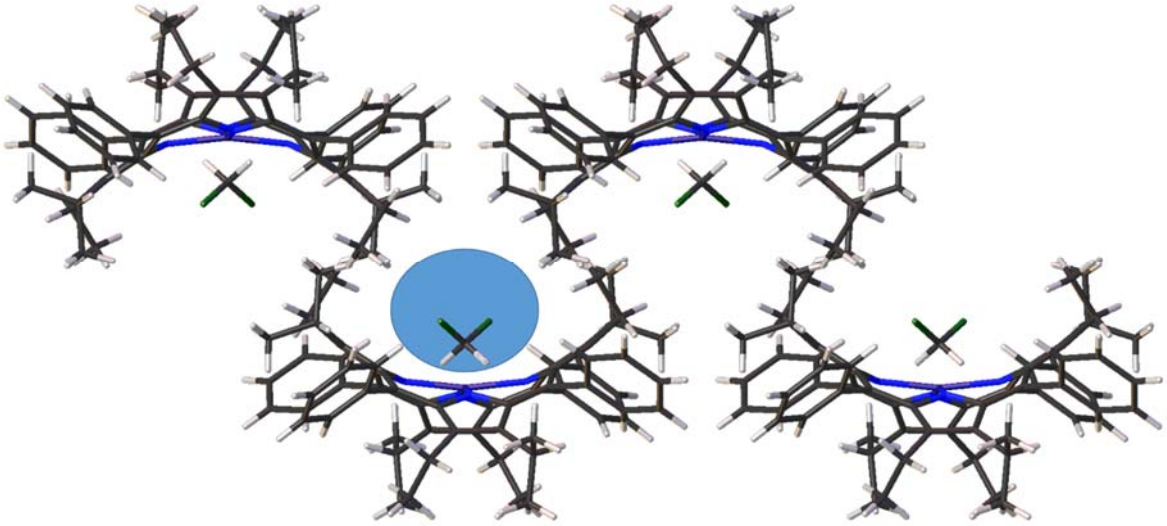

Figure 3: Excerpt of the crystal structure lattice diagram (stick model) of 16•DCM.[23a] The blue circle marks a hydrophobic binding pocket.

The selective formation of **15**•2HCl confirmed the initial hypothesis that the rational choice of the pyrrole and aldehyde components would open a new avenue to regioisomerically pure type I porphyrins via simple condensation pathways. In order to expand the product library, **14** was also reacted with 4-methoxybenzaldehyde with a similar outcome (Scheme 3).

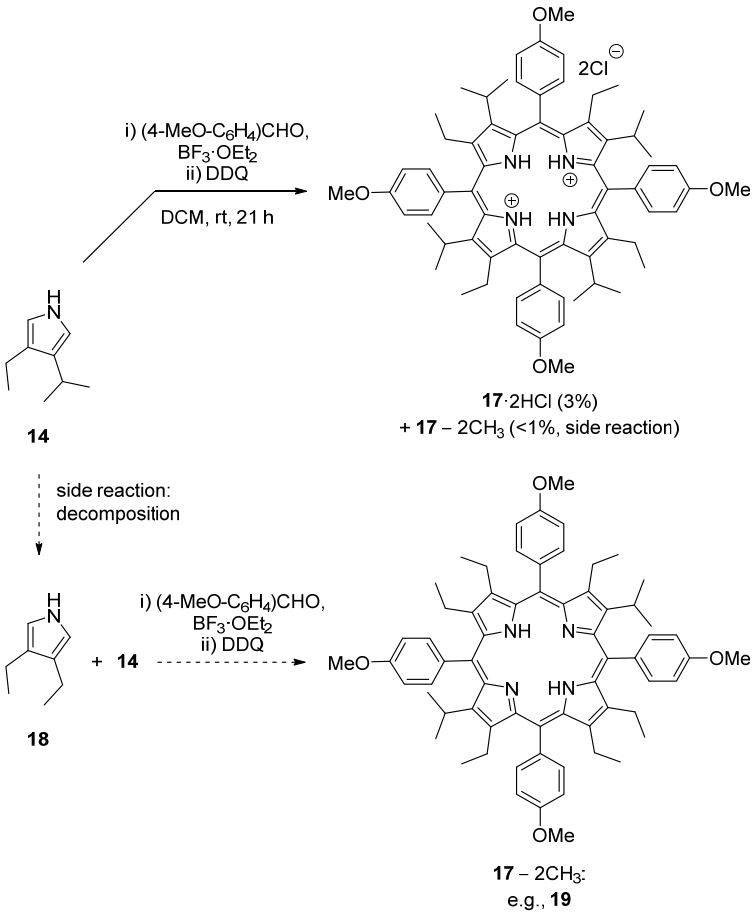

Scheme 3. Synthesis of the type I porphyrin 17•2HCl through a condensation reaction.

While the only porphyrin type isomer that could be observed and isolated was **17**•2HCl, the presence of another species after the condensation reaction was noted. This tetrapyrrole could be readily separated from **17**•2HCl, but no structure was assigned with ultimate certainty. However, HRMS analysis indicated that this porphyrin was devoid of two CH_3 fragments (**17** − $2CH_3$) when compared to **17**. Probably, a fraction of **14** underwent a type of dealkylation prior to condensation to form 3,4-diethylpyrrole (**18**), which could then have reacted with unaltered **14** and 4-methoxybenzaldehyde to form a tetrapyrrole like **19** or corresponding regioisomers (Scheme **3**). In any case, this side product could be separated from **17**•2HCl through conventional column chromatography and unambiguous assignment of the structure is currently under investigation.

In the following, it was attempted to extend this method to different types of pyrroles and to investigate some of the limitations. For this, 3-methyl-4-phenylpyrrole (**23**) was selected as a promising target in order to test whether it would be possible to introduce

aromatic functions into the β-positions of type I porphyrins. In practical terms, **23** was synthesized from **20** and toluenesulfonylmethyl isocyanide (**21**) in a sequence of a Van Leusen reaction[24] and a reduction of the methyl ester function in **22** (Scheme 4). Unfortunately, the condensation of **23** with benzaldehyde resulted in the formation of an inseparable statistical mixture of all four porphyrin isomers. Apparently, the difference in steric bulk between the methyl and phenyl group in **23** was not distinct enough for selective type I porphyrin formation. While the 4-phenyl substituent in **23** may be considered as a large functional group, the flat geometry of this group may account for an insufficient distinction from the 3-methyl unit in terms of bulkiness and, consequently, the lack of regioselectivity. This was reflected by a high number of methyl signals in the ^{1}H NMR spectra of the free base products and the corresponding Ni(II) complexes. The Ni(II) complexes were synthesized to investigate whether a separation by chromatography could be attempted, but TLC analysis indicated all too similar polarities. However, this example did not eliminate the option that in the future, 3,4-disubstituted pyrroles with more sterically demanding aromatic substituents may eventually lead to type I porphyrin formations.

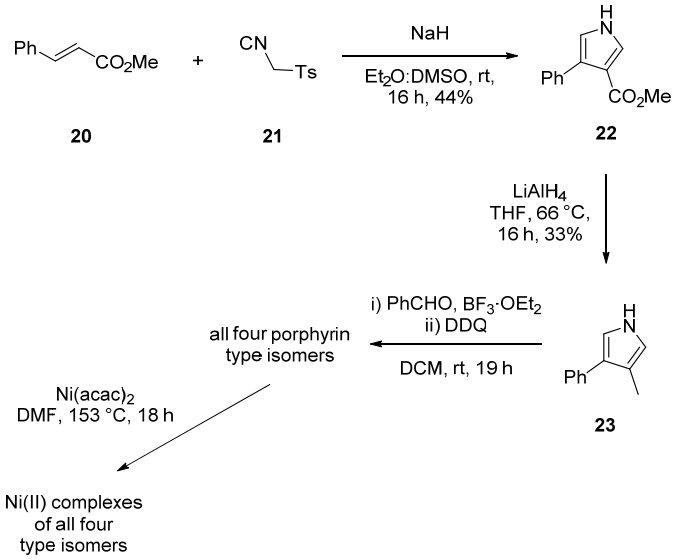

Scheme 4: Synthesis of 3-methyl-4-phenylpyrrole (23), acid-catalyzed condensation with benzaldehyde, and metallation.

Upon recrystallization of the pyrroles **14** and **23**, samples that were suitable for single crystal X-ray analysis could be obtained. The structural analysis revealed the formation of intermolecular H-bonds in both species between the polarized carbonyl

functions and N−H groups (Figure 4). This was an interesting observation since H-bonding of the nitrogenous hydrogen atoms in pyrroles is an important feature for the application as catalysts[4,25] and innovative sensors.[26]

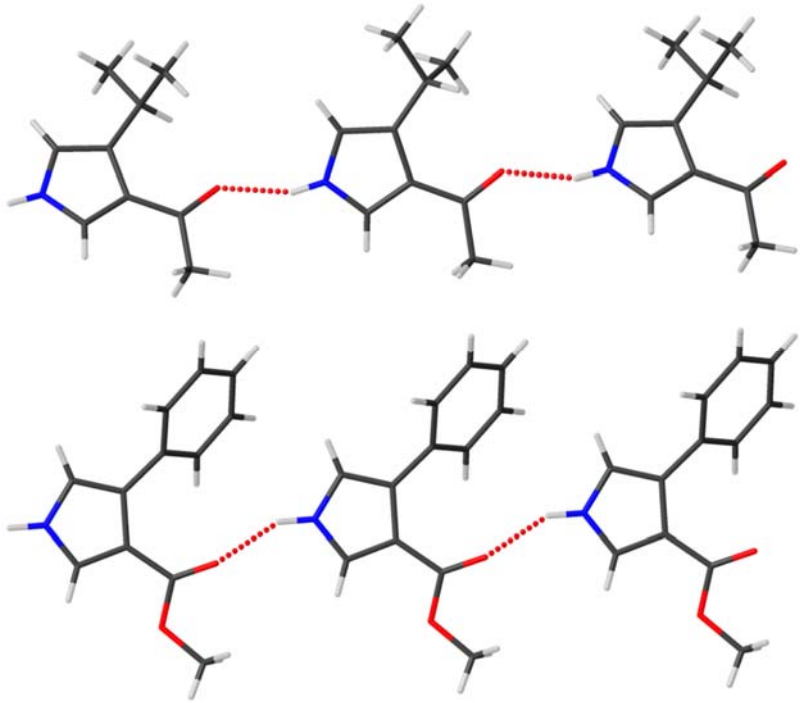

Figure 4: Excerpts of the crystal structure lattice diagrams (stick models) of 14 (top) and 23 (bottom), both revealing the formation of intermolecular H-bonds.[23a]

To conclude, a method for the selective preparation of type I porphyrins in straightforward condensation reactions was developed, and the utility of the method could be proven in a promising case study. Therein, dodecasubstituted type I porphyrins formed as the only regioisomers, and it is likely that the presence of a higher number of repulsive *peri*-interactions in the type II, III, and IV tetrapyrroles is responsible for the high degree of regioselectivity. Notably, this innovative method does not depend on tedious precursor syntheses, cumbersome purification steps (i.e., HPLC), or impractical limitations on the reaction scale that are usually associated with this type of chemistry. While this strategy was initially investigated for 3,4-dialkylpyrroles, an expansion to more diverse systems is currently under investigation. Moreover, the crystal structural analyses of **15**•2HCl and **16** confirmed the type I substitution pattern, likewise revealing a high degree of saddle distortion in both.

Interestingly, the Ni(II) complex **16** formed a tunnel-like structure in the solid state and acted as a receptor for DCM, which could be exploited for the sensing of neutral molecules in the future. Additionally, the crystal structures of the unsymmetrically 3,4-difunctionalized pyrroles **14** and **23**, which formed intermolecular H-bonds due to the presence of carbonyl and N−H groups, were solved, pointing at a potential as sensors and organocatalysts.

EXPERIMENTAL SECTION

Analytical Techniques. Analytical TLC was performed using sheets precoated with silica gel to a depth of 0.2 mm or aluminum oxide plates, both impregnated with fluorescence indicator F_{254}. The visualization was accomplished with a UV lamp. Flash column chromatography was carried out using aluminum oxide (neutral, activated with 6% H_2O, Brockman Grade III). Mass spectrometry analysis was performed with a Q-Tof Premier Waters MALDI quadrupole time-of-flight (Q-TOF) mass spectrometer equipped with a matrix-assisted laser desorption ionization (MALDI) source and DCTB (*trans*-2-[3-(4-*tert*-butylphenyl)-2-methyl-2-propenylidene]malononitrile) as the matrix. APCI experiments were performed on a Bruker microTOF-Q III spectrometer interfaced to a Dionex UltiMate 3000 LC. UV–vis absorption measurements were performed in DCM as the solvent using a Shimadzu MultiSpec-1501. Melting points are uncorrected and were measured with a Stuart SMP-50 melting point apparatus. ^{1}H and ^{13}C $\{^{1}H\}$ NMR spectra were recorded at 400.13 MHz and 100.61 MHz, respectively, using Bruker DPX400, Bruker AV 600, and Bruker AV 400 devices, respectively. All NMR experiments were performed at 25 °C. Resonances δ are given in ppm units and referenced to the deuterium peak in the NMR solvent $CDCl_3$ (δ_H = 7.26 ppm, δ_C = 77.2 ppm). Signal multiplicities are abbreviated as follows: singlet = s, doublet = d, quartet = q, septet = sept, multiplet = m. IR spectra were recorded on a PerkinElmer Spectrum 100 FTIR spectrometer utilizing the ATR sampling technique.

General Information. To protect air and moisture sensitive compounds, the corresponding reactions were carried out under “Schlenk” conditions using argon as an inert gas. Air and residual moisture were removed from the instruments by a hot air

gun under high vacuum, and the flasks were purged with argon subsequently. This cycle was repeated up to three times as necessary.

In the NMR spectra of the new highly substituted type I porphyrins, the signals corresponding to the β-ethyl and β-isopropyl groups are broad. This is in accordance with conformational studies by Medforth et al. on decaalkylporphyrins.[27] Presumably, the highly substituted products existed as a mixture of atropisomers in solution. The missing signals corresponding to the inner protons, as observed in most ^{1}H NMR spectra, have been reported previously, too.[28]

Materials. Most commercially available reagents were used as received unless otherwise noted. For example, THF and DCM for air and moisture sensitive reactions were obtained by passing the degassed solvents through an activated aluminium oxide column. Alternatively, DCM for porphyrin syntheses was obtained via drying over phosphorus pentoxide and distillation. The pyrroles **13**,[29] **22**,[30] and **23**[31] have been prepared following the literature.

3-Ethyl-4-isopropylpyrrole 14: 3-Acetyl-4-isopropylpyrrole **13** (4 g, 26.5 mmol, 1 equiv) in 70 mL THF was added dropwise to a suspension of $LiAlH_4$ (3.14 g, 82.7 mmol, 3.1 equiv) in 20 mL THF at 0 °C. After that, the reaction mixture was left to stir for 1 h at rt and heated to 66 °C for 17 h by an oil bath. Upon the careful hydrolysis with ≈150 mL of a 2 M sodium hydroxide solution at 0 °C, Et_2O was added, and the layers were separated. The aqueous phase was extracted with Et_2O, and the combined organic layers were washed with water, dried with $MgSO_4$, filtered, and the solvent was removed in vacuo. The title compound was obtained as yellow oil (3.05 g, 22.26 mmol, 84%). R_f 0.55 (SiO_2, hexane). ^{1}H NMR ($CDCl_3$, 400.13 MHz): δ 1.36–1.42 (m, 9H), 2.68 (q, J = 7.5 Hz, 2H), 3.02 (sept, J = 6.8 Hz, 1H), 6.65 (d, J = 2.7 Hz, 2H), 7.91 (s, 1H). ^{13}C {^{1}H} NMR ($CDCl_3$, 100.61 MHz): δ 14.6, 18.5, 24.0, 25.2, 113.3, 114.6, 124.0, 129.8. HRMS−APCI (*m*/*z*): $[M + H]^+$ calcd for $C_9H_{16}N$, 138.1277; found, 138.1281. MS–APCI *m*/*z* (% relative intensity, ion): 96.07 (100, M − C_3H_7 + 2H). IR (ATR) $\tilde{\nu}_{max}$: 2959, 2931, 2870, 1670, 1640, 1462, 1379, 1076, 896, 776 cm^{-1}.

2,7,12,17-Tetraethyl-3,8,13,18-tetraisopropyl-5,10,15,20-tetraphenyl-22*H*,24*H*-porphyrindiium dihydrochloride 15•2HCl: 3-Ethyl-4-isopropylpyrrole (**14**, 1 g, 7.29

mmol, 1 equiv) and benzaldehyde (0.77 g, 7.29 mmol, 1 equiv) were dissolved in dry DCM (1 L) and boron trifluoride diethyl etherate (90 μL, 0.73 mmol, 10 mol %) was added. This was reacted for 22 h at rt, followed by the addition of DDQ (7.28 g, 32.1 mmol, 4.4 equiv). The solution became purple and was left to stir for another hour. The solvent was removed at reduced pressure, the residue was dissolved in DCM and filtered through a plug of Al_2O_3, Brockman grade III, using DCM, mixtures of DCM and ethyl acetate, and eventually mixtures of ethyl acetate and methanol to partly separate the relevant green fractions. These were evaporated to dryness and chromatographed on Al_2O_3, Brockman grade III, using DCM:ethyl acetate, 2:1, v/v. A major green band was isolated, which contained the title compound. After drying in vacuo, **15**•2HCl was obtained as green solid (172 mg, 0.66 mmol, 9%). mp > 300 °C. R_f 0.34 (Al_2O_3, DCM:ethyl acetate, 10:1, v/v). ^{1}H NMR ($CDCl_3$, 400.13 MHz): δ −0.34 (s, 4H), −0.17–0.58 (m, 24H), 1.38–1.55 (m, 12H), 2.12–2.33 (m, 4H), 2.41–2.74 (m, 8H), 7.73–7.98 (m, 12H), 8.39–8.72 (m, 8H). ^{13}C {^{1}H} NMR ($CDCl_3$, 100.61 MHz): δ 14.7, 15.9, 16.4, 16.5, 16.6, 16.7 (× 3), 19.6 (× 2), 19.8, 23.0, 23.1, 23.2 (× 2), 23.3 (× 2), 27.4, 27.5, 32.2, 118.1, 118.2, 118.5, 118.7 (× 2), 118.8, 119.1, 128.7, 128.8, 128.9 (× 2), 129.0 (× 2), 129.1, 130.0 (× 2), 130.1, 130.7, 134.3, 137.3, 137.4 (× 2), 137.6, 137.7, 137.8 (× 2), 137.9 (× 2), 138.4, 138.7, 138.9, 139.1 (× 2), 139.2, 139.3, 139.5, 139.7, 139.9, 140.2, 140.8, 140.9, 141.1, 141.2 (× 2), 141.5, 144.9, 145.0 (× 2), 145.1, 145.2, 145.4, 145.5, 145.6, 145.7 (× 2), 145.8, 145.9, 146.0, 146.2. UV–vis (DCM) λ_{max} (log ε): 484 (5.57), 646 (4.09), 703 nm (4.69). HRMS−MALDI (*m*/*z*): $[M - 2HCl + H]^+$ calcd for $C_{64}H_{71}N_4$, 895.5673; found, 895.5670.

2,7,12,17-Tetraethyl-3,8,13,18-tetraisopropyl-5,10,15,20-tetraphenylporphyrinato}nickel(II) 16: Porphyrin **15**•2HCl (60.3 mg, 62 μmol, 1 equiv) and $Ni(acac)_2$ (159 mg, 0.62 mmol, 10 equiv) were dissolved in 0.6 mL DMF, and this was heated to 153 °C for 20 h by a heating mantle during which the reaction mixture changed color from green to purple. After cooling to rt, water and DCM were added, and the layers were separated. The aqueous phase was extracted with DCM and the combined organic layers were washed with water, dried with $MgSO_4$, filtered, and the solvent was evaporated in vacuo. The purple crude product was purified by column chromatography (Al_2O_3, Brockman grade III, using DCM:petroleum ether, 1:10, v/v). The first fraction, a purple band, was isolated and upon evaporation of the

solvent, the title compound was obtained as purple solid (51 mg, 53.3 µmol, 86%). mp > 300 °C. R_f 0.61 (SiO_2, hexane:DCM, 5:1, v/v). ^{1}H NMR ($CDCl_3$, 400.13 MHz): δ 0.33–0.49 (m, 12H), 0.54–0.77 (m, 12H), 1.26–1.45 (m, 12H), 1.79–2.09 (m, 4H), 2.52–2.83 (m, 8H), 7.53–7.70 (m, 12H), 7.94–8.21 (m, 8H). ^{13}C {^{1}H} NMR ($CDCl_3$, 100.61 MHz): δ 17.6, 20.4, 23.2, 26.7, 26.8, 26.9, 127.0, 127.3, 127.7, 127.8, 127.9, 128.1, 134.2, 134.7, 135.3, 140.7, 146.3, 146.5, 148.7, 148.9. UV–vis (DCM) λ_{max} (log ε): 444 (5.33), 593 (4.15), 599 nm (4.01). HRMS−MALDI (*m*/*z*): [M]$^+$ calcd for $C_{64}H_{68}N_4Ni$, 950.4797; found, 950.4785.

2,7,12,17-Tetraethyl-3,8,13,18-tetraisopropyl-5,10,15,20-tetrakis(4-methoxyphenyl)-22*H*,24*H*-porphyrindiium dihydrochloride 17•2HCl:

Similar to the synthesis of **15**•2HCl, 3-ethyl-4-isopropylpyrrole (**14**, 0.5 g, 3.6 mmol, 1.1 equiv) and 4-methoxybenzaldehyde (0.4 mL, 3.3 mmol, 1 equiv) were dissolved in 500 mL of dry DCM and BF_3•OEt_2 (43 μL, 0.33 mmol, 10 mol %) was added. This was reacted at rt for 21 h during which the reaction mixture turned red, followed by DDQ addition (3.3 g, 14.52 mmol, 4.4 equiv). After stirring for another 2 h, the solvent was removed in vacuo and the residue dissolved in DCM and filtered through Al_2O_3, Brockman grade IIII, using DCM and DCM:ethyl acetate mixtures up to pure ethyl acetate to remove DDQ derivatives and other nonporphyrin material. Then, DCM:methanol, 1:1, v/v was applied to isolate a green/brown fraction. The relevant fractions, which had brown or green/brown colors, were combined upon TLC analysis, and the solvent was evaporated. The crude product was then subjected to column chromatography. Column chromatography (Al_2O_3, Brockman grade IIII) was performed using DCM to remove brown impurities, then DCM:ethyl acetate, 10:1, v/v to isolate a light green fraction of **17**•2HCl, giving a green solid (27 mg, 0.1 mmol, 3%) upon evaporation of the solvent. Second, a porphyrin (e.g., **19**, see Scheme 3) that was devoid of two CH_3 fragments when compared to **17**, as indicated by HRMS analysis, was eluted as a dark green band, yielding a green solid (5 mg, <1%) after evaporation of the solvent. **17**•2HCl: mp 286–290 °C dec. R_f 0.67 (Al_2O_3, DCM:ethyl acetate, 10:1, v/v). ^{1}H NMR ($CDCl_3$, 400.13 MHz): δ 0.02–0.24 (m, 12H), 0.25–0.38 (m, 12H), 1.44–1.54 (m, 12H), 2.21–2.39 (m, 4H), 2.44–2.71 (m, 8H), 4.09 (s, 3H), 4.11 (s, 6H), 4.12 (s, 3H), 7.35–7.44 (m, 8H) 8.31–8.55 (m, 8H). ^{13}C {^{1}H} NMR ($CDCl_3$, 100.61 MHz): δ 15.7, 15.8, 15.9 (× 2), 16.0, 19.1, 26.6, 26.7, 113.7, 114.1 (× 2), 116.6,

116.8, 117.2, 117.4, 117.7, 118.0, 130.4, 131.5, 131.8, 132.7, 133.0, 137.5, 137.8, 137.9, 138.0, 138.1, 138.4, 138.5 (× 2), 138.6, 139.6, 139.7, 140.0, 140.5, 144.8, 144.9, 145.0, 145.3, 145.4, 145.6, 145.7, 145.8, 146.0, 146.3, 146.5, 161.0, 161.1. UV–vis (DCM) λ_{max} (log ε): 486 (5.63), 722 nm (4.87). HRMS−MALDI (*m*/*z*): [M − H − 2Cl]$^+$ calcd for $C_{68}H_{79}N_4O_4$, 1015.6101; found, 1015.6074. **17** − $2CH_3$ (e.g., **19**): HRMS−MALDI (*m/z*): [M − 2HCl + H]$^+$ calcd for $C_{62}H_{67}N_4$, 867.5360; found, 867.5371.

Crystal Structure Determinations. Crystals were grown following the protocol developed by Hope, by dissolving the compounds in DCM, layering with methanol or hexane and allowing for slow diffusion over time.[32] This was aided by slow evaporation once the layers had mixed completely. Diffraction data for all compounds were collected on a Bruker APEX 2 DUO CCD diffractometer by using graphite-monochromated MoK_α radiation (λ = 0.71073 Å) and Incoatec IμS CuK_α radiation (λ = 1.54178 Å). Crystals were mounted on a MiTeGen MicroMount and collected at 297(2) or 100(2) K by using an Oxford Cryosystems Cobra low-temperature device. Data were collected by using omega and phi scans and were corrected for Lorentz and polarization effects by using the APEX software suite.[33] The structures were solved with Direct Methods and refined against $|F^2|$ with XL using least squares minimization.[23b,34] Non-hydrogen atoms were refined with anisotropical thermal parameters. Hydrogen atoms were generally placed into geometrically calculated positions and refined using a riding model. The N–H hydrogen atoms were located using difference maps and refined using the standard riding model. All images were prepared by using Olex2.[23b]

Crystal data for 3-acetyl-4-isopropylpyrrole 13: $C_9H_{13}NO$, M = 151.20, monoclinic, $P2_1/c$, a = 9.0803(8) Å, b = 6.7468(6), c = 14.6471(12) Å, V = 896.83(13) Å^3, T = 100(2) K, Z = 4, μ(Cu$K\alpha$) = 0.073, 18366 reflections measured, 2065 unique (R_{int} = 0.0484) which were used in all calculations. The final wR_2 was 0.1115 (all data) and R_1 was 0.0449 ($I > 2\sigma(I)$).

Crystal data for 2,7,12,17-tetraethyl-3,8,13,18-tetraisopropyl-5,10,15,20-tetraphenyl-22*H*,24*H*-porphyrindiium dihydrochloride 15•2HCl: $C_{64}H_{72}Cl_2N_4$, M = 968.15, cubic, *I*-43*d*, a = 27.1155(7) Å, V = 19936.7(15) Å^3, T = 100(2) K, Z = 12,

μ(CuK$_\alpha$) = 1.142, 93602 reflections measured, 2041 unique (R_{int} = 0.1481) which were used in all calculations. The final wR_2 was 0.21116 (all data) and R_1 was 0.0718 ($I > 2\sigma(I)$).

Crystal data for {2,7,12,17-tetraethyl-3,8,13,18-tetraisopropyl-5,10,15,20-tetraphenylporphyrinato}nickel(II) 16•DCM: $C_{65}H_{70}Cl_2N_4Ni$, M = 1036.86, tetragonal, $P4_2/n$, a = 14.6097(5) Å, c = 15.4733(5) Å, V = 3302.7(2) Å^3, T = 100(2) K, Z = 2, μ(CuKα) = 1.443, 70820 reflections measured, 2906 unique (R_{int} = 0.0495) which were used in all calculations. The final wR_2 was 0.2208 (all data) and R_1 was 0.0770 ($I > 2\sigma(I)$).

Crystal data for methyl 4-phenylpyrrole-3-carboxylate 22: $C_{12}H_{11}NO_2$, M = 201.22, monoclinic, $P12_1/n1$, a = 7.0408(10) Å, b = 9.2884(13), c = 16.116(3) Å, V = 1046.7(3) Å^3, T = 297(2) K, Z = 4, μ(CuKα) = 0.088, 11142 reflections measured, 2629 unique (R_{int} = 0.0349) which were used in all calculations. The final wR_2 was 0.1339 (all data) and R_1 was 0.0470 ($I > 2\sigma(I)$).

ACKNOWLEDGMENTS

This work was supported by grants from Science Foundation Ireland (SFI IvP 13/IA/1894) and through funding from the European Union's Horizon 2020 research and innovation program under the FET Open grant agreement no. 828779.

SUPPORTING INFORMATION

^{1}H and ^{13}C NMR spectra of the newly synthesized compounds, single crystal X-ray structures, and ^{1}H NMR spectra of statistical porphyrin type isomer mixtures. This material is available free of charge via the Internet at http://pubs.acs.org. CCDC 1993404–1993407 contain the supplementary crystallographic data for this note. These data can be obtained free of charge from The Cambridge Crystallographic Data Centre (CCDC) *via* www.ccdc.cam.ac.uk/data_request/cif.

REFERENCES

(1) Huber, R. “A structural basis of light energy and electron transfer in biology”, *Eur. J. Biochem*. **1990**, *187*, 283–305.
(2) (*a*) Senge, M. O.; MacGowan, S. A.; O'Brien, J. M. “Conformational control of cofactors in nature – the influence of protein-induced macrocycle distortion on the biological function of tetrapyrroles”, *Chem. Commun*. **2015**, *51*, 17031–17063; (*b*) Senge, M. O. “N-H Hydrogen Bonding in Porphyrins - from Conformational Design to Supramolecular Chemistry”, *ECS Trans*. **2015**, *66*, 1–10.
(3) (*a*) Kielmann, M.; Prior, C.; Senge, M. O. “Porphyrins in troubled times: a spotlight on porphyrins and their metal complexes for explosives testing and CBRN defense”, *New J. Chem*. **2018**, *42*, 7529–7550; (*b*) Ding, Y.; Zhu, W.-H.; Xie, Y. “Development of Ion Chemosensors Based on Porphyrin Analogues”, *Chem. Rev*. **2017**, *117*, 2203–2256; (*c*) Zou, Q.; Abbas, M.; Zhao, L.; Li, S.; Shen, G.; Yan, X. “Biological Photothermal Nanodots Based on Self-Assembly of Peptide–Porphyrin Conjugates for Antitumor Therapy”, *J. Am. Chem. Soc*. **2017**, *139*, 1921–1927; (*d*) Rawson, J.; Stuart, A. C.; You, W.; Therien, M. J. “Tailoring Porphyrin-Based Electron Accepting Materials for Organic Photovoltaics”, *J. Am. Chem. Soc*. **2014**, *136*, 17561–17569; (*e*) Ethirajan, M.; Chen, Y.; Joshi, P.; Pandey, R. K. “The role of porphyrin chemistry in tumor imaging and photodynamic therapy”, *Chem. Soc. Rev*. **2011**, *40*, 340–362; (*f*) Senge, M. O. “Stirring the porphyrin alphabet soup—functionalization reactions for porphyrins”, *Chem. Commun*. **2011**, *47*, 1943–1960.
(4) (*a*) Kielmann, M.; Senge, M. O. “Molekulares Engineering freier Porphyrinbasen als Liganden – das N-H···X-Bindungsmotiv in Tetrapyrrolen”, *Angew. Chem*. **2019**, *131*, 424–448; “Molecular Engineering of Free-Base Porphyrins as Ligands—The N−H···X Binding Motif in Tetrapyrroles”, *Angew. Chem. Int. Ed*. **2019**, *58*, 418–441; (*b*) Kielmann, M.; Grover, N.; Kalisch, W. W.; Senge, M. O. “Incremental Introduction of Organocatalytic Activity into Conformationally Engineered Porphyrins”, *Eur. J. Org. Chem*. **2019**, 2448–2452; (*c*) Roucan, M.; Kielmann, M.; Connon, S. J.; Bernhard, S. S. R.; Senge, M. O. “Conformational control of nonplanar free base porphyrins: towards bifunctional catalysts of tunable basicity”, *Chem. Commun*. **2018**, *54*, 26–29.
(5) (*a*) Zhang, J.-X.; Chan, W.-L.; Xie, C.; Zhou, Y.; Chau, H.-F.; Maity, P.; Harrison, G. T.; Amassian, A.; Mohammed, O. F.; Tanner, P. A.; Wong, W.-K.; Wong, K.-L. “Impressive near-infrared brightness and singlet oxygen generation from strategic

lanthanide–porphyrin double-decker complexes in aqueous solution", *Light Sci. Appl*. **2019**, *8*, No. 46; (*b*) Callaghan, S.; Senge, M. O. "The good, the bad, and the ugly – controlling singlet oxygen through design of photosensitizers and delivery systems for photodynamic therapy", *Photochem. Photobiol. Sci*. **2018**, *17*, 1490–1514; (*c*) Chen, Y.-Z.; Wang, Z. U.; Wang, H.; Lu, J.; Yu, S.-H.; Jiang, H.-L. "Singlet Oxygen-Engaged Selective Photo-Oxidation over Pt Nanocrystals/Porphyrinic MOF: The Roles of Photothermal Effect and Pt Electronic State", *J. Am. Chem. Soc*. **2017**, *139*, 2035–2044.

(6) Norvaiša, K.; Flanagan, K. J.; Gibbons, D.; Senge, M. O. "Konformativer Umbau von Porphyrinen als Rezeptoren mit schaltbaren N-H···X-Bindungsmodi", *Angew. Chem*. **2019**, *131*, 16705–16709; "Conformational Re-engineering of Porphyrins as Receptors with Switchable N−H···X-Type Binding Modes", *Angew. Chem. Int. Ed*. **2019**, *58*, 16553–16557.

(7) (*a*) Kielmann, M.; Flanagan, K. J.; Norvaiša, K.; Intrieri, D.; Senge, M. O. "Synthesis of a Family of Highly Substituted Porphyrin Thioethers via Nitro Displacement in 2,3,7,8,12,13,17,18-Octaethyl-5,10,15,20-tetranitroporphyrin", *J. Org. Chem*. **2017**, *82*, 5122–5134; (*b*) Meindl, A.; Plunkett, S.; Ryan, A. A.; Flanagan, K. J.; Callaghan, S.; Senge, M. O. "Comparative Synthetic Strategies for the Generation of 5,10- and 5,15-Substituted *Push-Pull* Porphyrins", *Eur. J. Org. Chem*. **2017**, 3565–3583; (*c*) Hiroto, S.; Miyake, Y.; Shinokubo, H. "Synthesis and Functionalization of Porphyrins through Organometallic Methodologies", *Chem. Rev*. **2017**, *117*, 2910–3043.

(8) Nguyen, L. T.; Smith, K. M. "Syntheses of type-I porphyrins via monopyrrole tetramerization", *Tetrahedron Lett*. **1996**, *37*, 7177–7180.

(9) Nguyen, L. T.; Senge, M. O.; Smith, K. M. "One-pot synthesis of regiochemically pure porphyrins from two different pyrroles", *Tetrahedron Lett*. **1994**, *35*, 7581–7584.

(10) Smith, K. M. "Porphyrins and bile pigments from brominated pyrromethenes", *J. Chem. Soc., Perkin Trans. 1* **1972**, 1471–1475.

(11) Paine III, J. B.; Chang, C. K.; Dolphin, D. "The Synthesis of Porphyrins *via* Dipyrromethenes", *Heterocycles* **1997**, *7*, 831–838.

(12) Lim, C. K.; Rideout, J. M.; Wright, D. J. "Separation of porphyrin isomers by high-performance liquid chromatography", *Biochem. J*. **1983**, *211*, 435–438.

(13) Fyrestam, J.; Bjurshammar, N.; Paulsson, E.; Johannsen, A.; Östman, C. “Determination of porphyrins in oral bacteria by liquid chromatography electrospray ionization tandem mass spectrometry”, *Anal. Bioanal. Chem*. **2015**, *407*, 7013–7023.
(14) Taniguchi, M.; Lindsey, J. S. “Enumeration of Isomers of Substituted Tetrapyrrole Macrocycles: From Classical Problems in Biology to Modern Combinatorial Libraries” in *Handbook of Porphyrin Science*; Kadish, K. M.; Smith, K. M.; Guilard, R., Eds.; World Scientific: Singapore, 2012; Vol. 23, pp. 1–80.
(15) Chu, T. C.; Chu, E. J.-H. “Porphyrin Patterns in Different Types of Porphyria”, *Clin. Chem*. **1967**, *13*, 371–387.
(16) Neya, S.; Funasaki, N. “*meso*-Tetra(*tert*-butyl)porphyrin as a precursor of porphine” *Tetrahedron Lett*. **2002**, *43*, 1057–1058.
(17) Neya, S.; Quan, J.; Hoshino, T.; Hata, M.; Funasaki, N. “Convenient synthesis of porphine from β-tetra(*tert*-butyl)porphyrin”, *Tetrahedron Lett*. **2004**, *45*, 8629–8630.
(18) Zakavi, S.; Omidyan, R.; Talebzadeh, S. “The influence of protonation on the structure and spectral properties of porphine: UV-vis, ^{1}H NMR and *ab initio* studies”, *RCS Adv*. **2016**, *6*, 82219–82226.
(19) Lindsey, J. S.; Schreiman, I. C.; Hsu, H. C.; Kearney, P. C.; Marguerettaz, A. M. “Rothemund and Adler-Longo reactions revisited: synthesis of tetraphenylporphyrins under equilibrium conditions”, *J. Org. Chem*. **1987**, *52*, 827–836.
(20) Hursthouse, M. B.; Neidle, S. “The crystal structure of 5-benzoyloxyoctaethylporphyrin. An example of a distorted porphyrin ring”, *J. Chem. Soc., Chem. Commun*. **1972**, 449–450.
(21) Senge, M. O. “Highly Substituted Porphyrins” in *The Porphyrin Handbook*; Kadish, K. M.; Smith, K. M.; Guilard, R., Eds.; Academic Press: New York, 2000; Vol. 1, pp. 239–348.
(22) Sparks, L. D.; Medforth, C. J.; Park, M.-S.; Chamberlain, J. R.; Ondrias, M. R.; Senge, M. O.; Smith, K. M.; Shelnutt, J. A. “Metal dependence of the nonplanar distortion of octaalkyltetraphenylporphyrins”, *J. Am. Chem. Soc*. **1993**, *115*, 581–592.
(23) (*a*) This figure was generated using Olex2;[23b] (*b*) Dolomanov, O. V.; Bourhis, L. J.; Gildea, R. J.; Howard, J. A. K.; Puschmann, H. “*OLEX2*: a complete structure solution, refinement and analysis program”, *J. Appl. Crystallogr*. **2009**, *42*, 339–341.
(24) Oldenziel, O. H.; Van Leusen, D.; Van Leusen, A. M. “Chemistry of sulfonylmethyl isocyanides. 13. A general one-step synthesis of nitriles from ketones using

tosylmethyl isocyanide. Introduction of a one-carbon unit", *J. Org. Chem*. **1977**, *42*, 3114–3118.
(25) Hirata, G.; Maeda, H. "Pyrrole-Based Anion-Responsive π-Electronic Molecules as Hydrogen-Bonding Catalysts", *Org. Lett*. **2018**, *20*, 2853–2856.
(26) Gale, P. A.; Sessler, J. L.; Camiolo, S. "Pyrrole- and Polypyrrole-Based Anion Receptors" in *Enzyclopedia of Supramolecular Chemistry*; Atwood, J. L.; Steed, J. W., Eds.; CRC Press: Boca Raton, FL, 2004; Vol. 2, pp. 1176–1185.
(27) Medforth, C. J.; Senge, M. O.; Forsyth, T. P.; Hobbs, J. D.; Shelnutt, J. A.; Smith, K. M. "Conformational Study of 2,3,5,7,8,12,13,15,17,18-Decaalkylporphyrins", *Inorg*. *Chem*. **1994**, *33*, 3865–3872.
(28) Watanabe, E.; Nishimura, S.; Ogoshi, H.; Yoshida, Z. "Orientation of electrophilic meso-substitution in metallooctaethylporphyrins" *Tetrahedron* **1975**, *31*, 1385–1390.
(29) Sugawara, S.; Kodama, M.; Hirata, Y.; Kojima, S.; Yamamoto, Y. "Synthesis and characterization of the most distorted 16π porphyrin: 16π octaisopropyltetraphenylporphyrin (OiPTPP)" *J. Porphyrins Phthalocyanines* **2011**, *15*, 1326–1334.
(30) van Leusen, A. M.; Siderius, H.; Hoogenboom, B. E.; van Leusen, D. "A new and simple synthesis of the pyrrole ring system from Michael acceptors and tosylmethylisocyanides", *Tetrahedron Lett*. **1972**, *13*, 5337–5340.
(31) Van Leusen, D.; Van Echten, E.; Van Leusen, A. M. "Chemistry of sulfonylmethyl isocyanides. 37. Synthesis of 3,4-disubstituted pyrroles bearing substituents of electron-withdrawing and/or electron-donating nature", *J. Org. Chem*. **1992**, *57*, 2245–2249.
(32) Hope, H. "X-Ray Crystallography: A Fast, First-Resort Analytical Tool" in *Progress in Inorganic Chemistry*; Karlin, K. D., Ed.; John Wiley & Sons, Inc.: Hoboken, NJ, 1994; Vol. 41, pp 1–19.
(33) (*a*) in *Saint*, Version 8.37a ed., Bruker AXS, Inc., Madison, WI, **2013**; (*b*) in *SADABS*, version 2016/2 ed., Bruker AXS, Inc, Madison, WI, **2014**; (*c*) in *APEX3*, Version 2016.9-0 ed., Bruker AXS, Inc., Madison, WI, **2016**.
(34) Sheldrick, G. M. "SHELXT – Integrated space-group and crystal-structure determination", *Acta Cryst. Sect. A* **2015**, *71*, 3–8.